Supplementary information

Quantitative assessment of the nature of noncovalent interactions in *N*-substituted-5-(adamantan-1-yl)-1,3,4-thiadiazole-2-amines: insights from crystallographic and QTAIM analysis

Ali A. El-Emam,[a] Elangovan Saveeth Kumar,[b] Krishnakumar Janani,[b] Lamya H. Al-Wahaibi,[c] Olivier Blacque,[d] Mohamed I. El-Awady,[e] Nora H. Al-Shaalan,[c] M. Judith Percino,[f] and Subbiah Thamotharan*[b]

[a]*Department of Medicinal Chemistry, Faculty of Pharmacy, Mansoura University, Mansoura 35516, Egypt*
[b]*Biomolecular Crystallography Laboratory, Department of Bioinformatics, School of Chemical and Biotechnology, SASTRA Deemed University, Thanjavur-613 401, India*
[c]*Department of Chemistry, College of Sciences, Princess Nourah bint Abdulrahman University, Riyadh 11671, Saudi Arabia*
[d]*Department of Chemistry, University of Zurich, Winterthurerstrasse 190, 8057 Zurich, Switzerland*
[e]*Department of Pharmaceutical Analytical Chemistry, Faculty of Pharmacy, Mansoura University, Mansoura 35516, Egypt*
[f]*Unidad de Polímeros y Electrónica Orgánica, Instituto de Ciencias, Benemérita Universidad Autónoma de Puebla, Val3-Ecocampus Valsequillo, Independencia O2 Sur 50, San Pedro Zacachimalpa, Puebla-C.P.72960, México*

Table of content

Synthesis of 1-(l-adamantylcarbonyl)-4-substituted thiosemicarbazides (A)[1,2]

The appropriate alkyl or arylisothiocyanate (0.01 mol) was added to a solution of adamantane-1-carboxylic acid hydrazide 1 (1.9 g, 0.01 mol) in ethanol (30 mL) and the mixture was heated under reflux for 1 h. On cooling, the precipitated solid was filtered, washed with ethanol and dried. The products were pure enough to be used in the next step without further purification.

Synthesis of *N*-substituted-5-(adamantan-1-yl)-1,3,4-thiadiazole-2-amines (I-III)[3]

Concentrated sulphuric acid (15 mL) was added dropwise to the appropriate thiosemicarbazide **A** (0.005 mol) and the mixture was stirred at ambient temperature for 24 h. The mixture was then poured into crushed ice (100 g) and the separated solid (in case of compounds **II** and **III**) was filtered, washed with dilute ammonium hydroxide solution and water, dried and crystallized from ethanol. In case of compound **I** the products were not precipitated upon addition to crushed ice and it was necessary to neutralize the mixture with ammonium hydroxide solution where the product was precipitated, washed with water, dried and crystallized from aqueous ethanol. Single crystals suitable for X-ray diffraction were obtained by slow evaporation of solution of the compounds in EtOH/$CHCl_3$ (1:2) at room temperature.

Compound **I**: M.p.: 168-170 °C; Yield: 66%. ^{1}H NMR ($CDC1_3$, 90 MHz): δ 1.20 (t, 3H, CH_3), 1.75 (s, 6H, Adamantane-H), 2.15 (s, 9H, Adamantyl-H), 3.20-3.50 (q, 2H, C***H***$_2CH_3$), 5.35 (s, 1H, NH, D_2O-exhang.).

Compound **II**: M.p.: 247-249 °C; Yield: 51%. ^{1}H NMR (DMSO-d_6, 90 MHz): δ 1.75 (s, 6H, Adamantane-H), 2.0 (s, 9H, Adamantyl-H), 7.05-7.30 (m, 2H, Ar-H), 7.50-7.75 (m, 2H, Ar-H), 10.25 (s, 1H, NH, D_2O-exhang.).

Compound **III**: M.p.: 263-265 °C; Yield: 55%. ^{1}H NMR (DMSO-d_6, 90 MHz): δ 1.75 (s, 6H, Adamantane-H), 2.05 (s, 9H, Adamantyl-H), 7.53-7.65 (m, 4H, Ar-H), 10.35 (s, 1H, NH, D_2O-exhang.).

1. A. A. E1-Emam and T. M. Ibrahim, *Arzneim.-Forsch./Drug Res.*, 1991, **41**,1260-1264.
2. O. A. Al-Deeb, M. A. Al-Omar, N. R. El-Brollosy, E. E. Habib, T. M. Ibrahim and A. A. El-Emam, *Arzneim.-Forsch./Drug Res.*, 2006, **56**, 40-47.
3. A. A. EI-Emam and J. Lehmann, *Monatsh. Chem.*, 1994, **125**, 587-591.

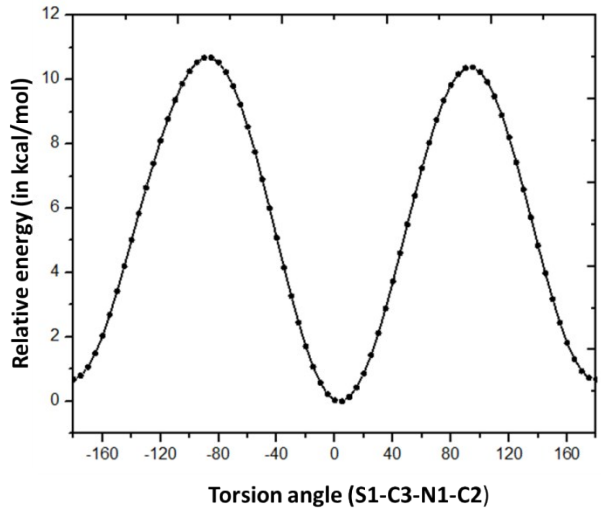

Fig. S1. PES for the S1-C3-N1-C2 torsion angle in **I**.

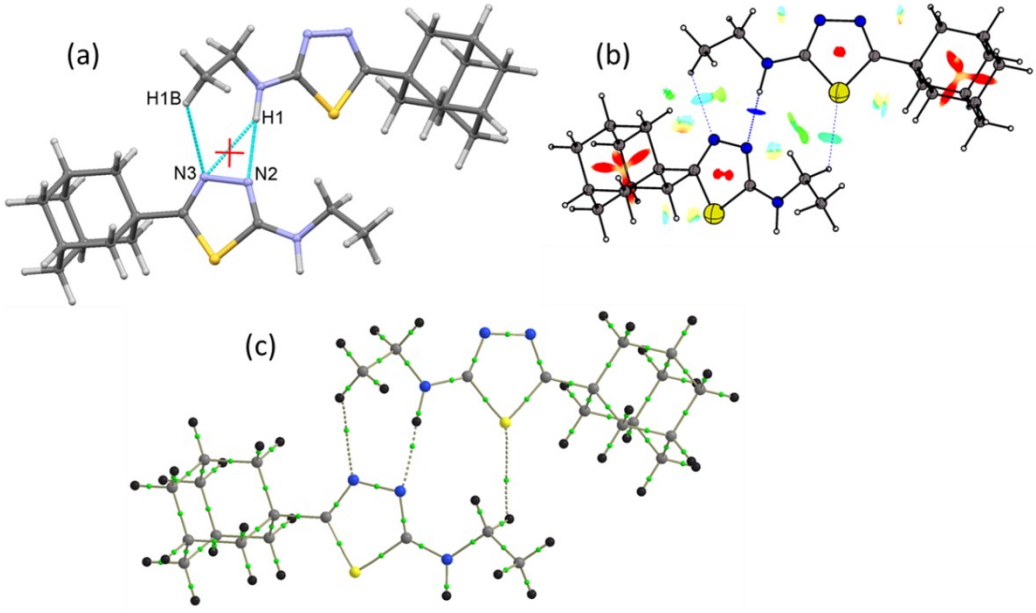

Fig. S2. Molecular dimer of M1 in **I**. (a) dimer of M1 and (b, c) NCI plot and molecular graph confirm the non-existence of N1–H1···N3 hydrogen bond.

Table S1. Topological parameters for intramolecular noncovalent interactions in **II**. These parameters were obtained from QTAIM analysis. R_{ij}: Bond path (Å), ρ(r): electron density

(e/Å^3); $\nabla^2\rho(r)$: Laplacian of electron density (e/Å^5); V(r): potential energy density (kJ mol^{-1} bohr^{-3}); G: kinetic energy density (kJ mol^{-1} bohr^{-3}). *D*e: dissociation energy = -V(r) × 0.5 (kcal mol^{-1}).

Interacting atoms	Bond path R_{ij}	$\rho(r)$	$\nabla^2\rho(r)$	V(r)	G(r)	H*(r)*	*De*
X-ray							
C3–H3···S1	2.599	0.099	1.174	-23.9	28.0	4.0	2.87

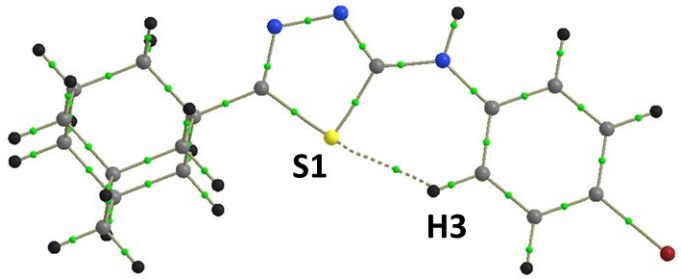

Fig. S3. Molecular graphs showing the formation of intramolecular C–H···S interaction in **II**.

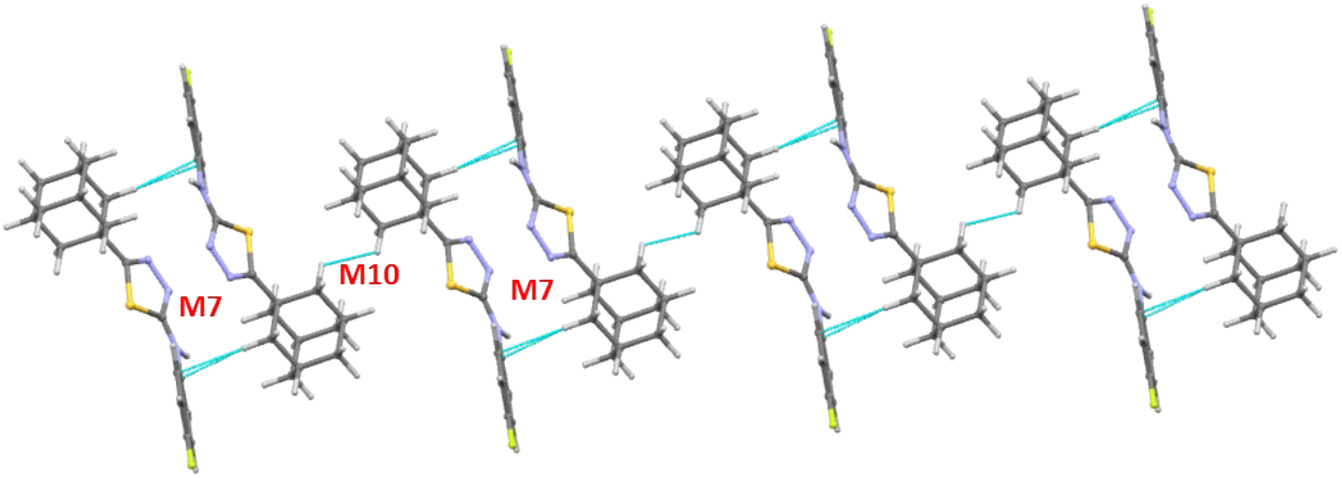

Fig. S4. Alternate M7 and M10 motifs generate molecular ribbons formed in **II**.

Table S2. Topological parameters for intramolecular noncovalent interactions in **III**. These parameters were obtained from QTAIM analysis. R_{ij}: Bond path (Å), $\rho(r)$: electron density

(e/Å^3); $\nabla^2\rho(r)$: Laplacian of electron density (e/Å^5); V(r): potential energy density (kJ mol^{-1} bohr^{-3}); G: kinetic energy density (kJ mol^{-1} bohr^{-3}). *De*: dissociation energy = -V(r) × 0.5 (kcal mol^{-1}).

Interacting atoms	Bond path R_{ij}	$\rho(r)$	$\nabla^2\rho(r)$	V(r)	G(r)	H*(r)*	*De*
X-ray							
C3–H3···S1	2.439	0.118	1.364	-30.2	33.7	3.5	3.63

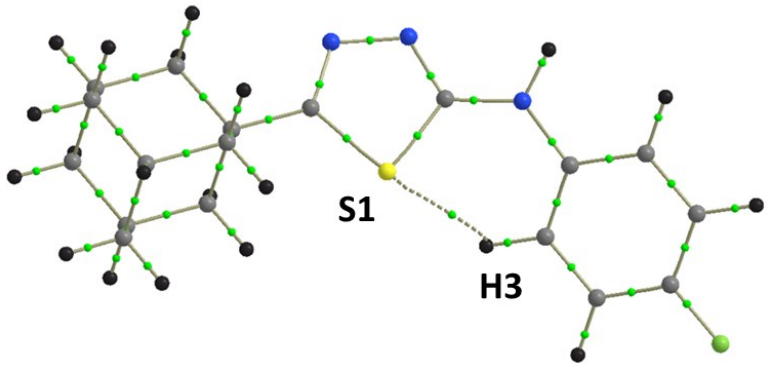

Fig. S5. Molecular graphs showing the formation of intramolecular C–H···S interaction in **III**.

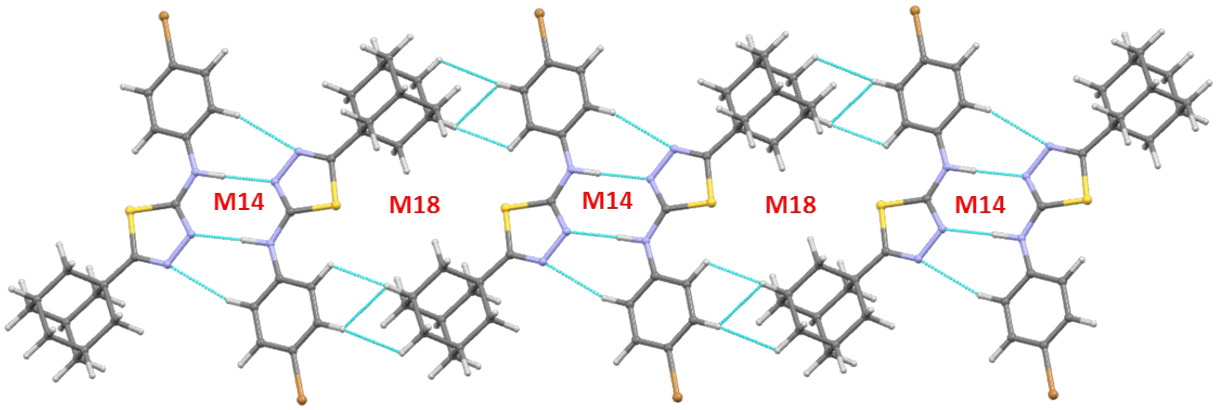

Fig. S6. Alternate motifs of M14 and M18 in **III** generate molecular sheet.

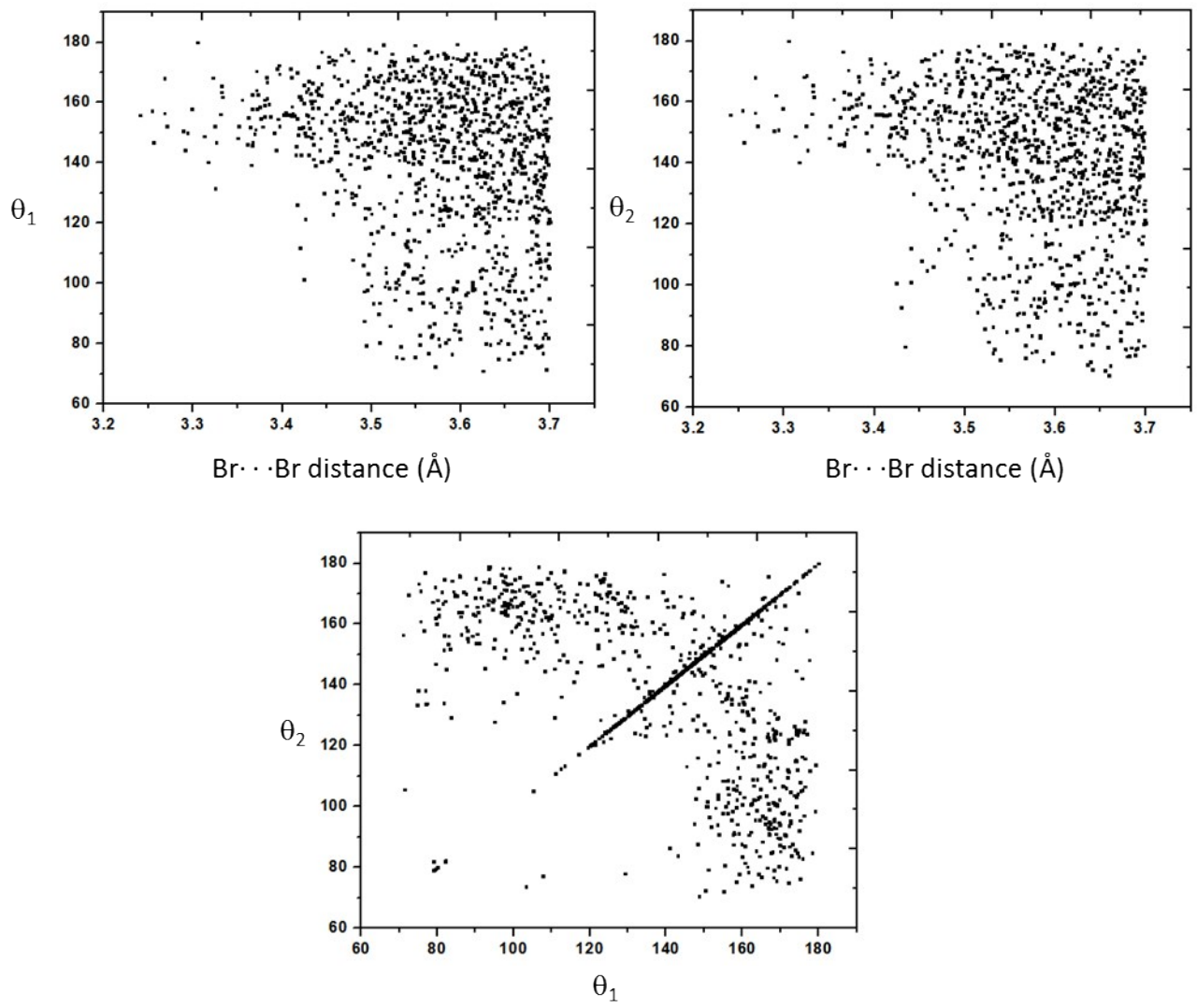

Fig. S7. Scatterplots showing the distribution of (a) Br···Br distance vs θ_1, (b) Br···Br distance vs θ_2 and (c) $\theta_1$vs θ_2.

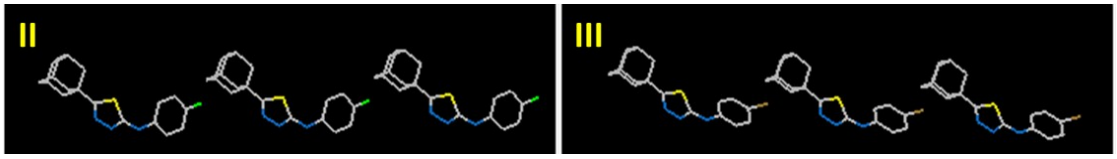

Fig. S8. Common packing features observed in **II** and **III**.

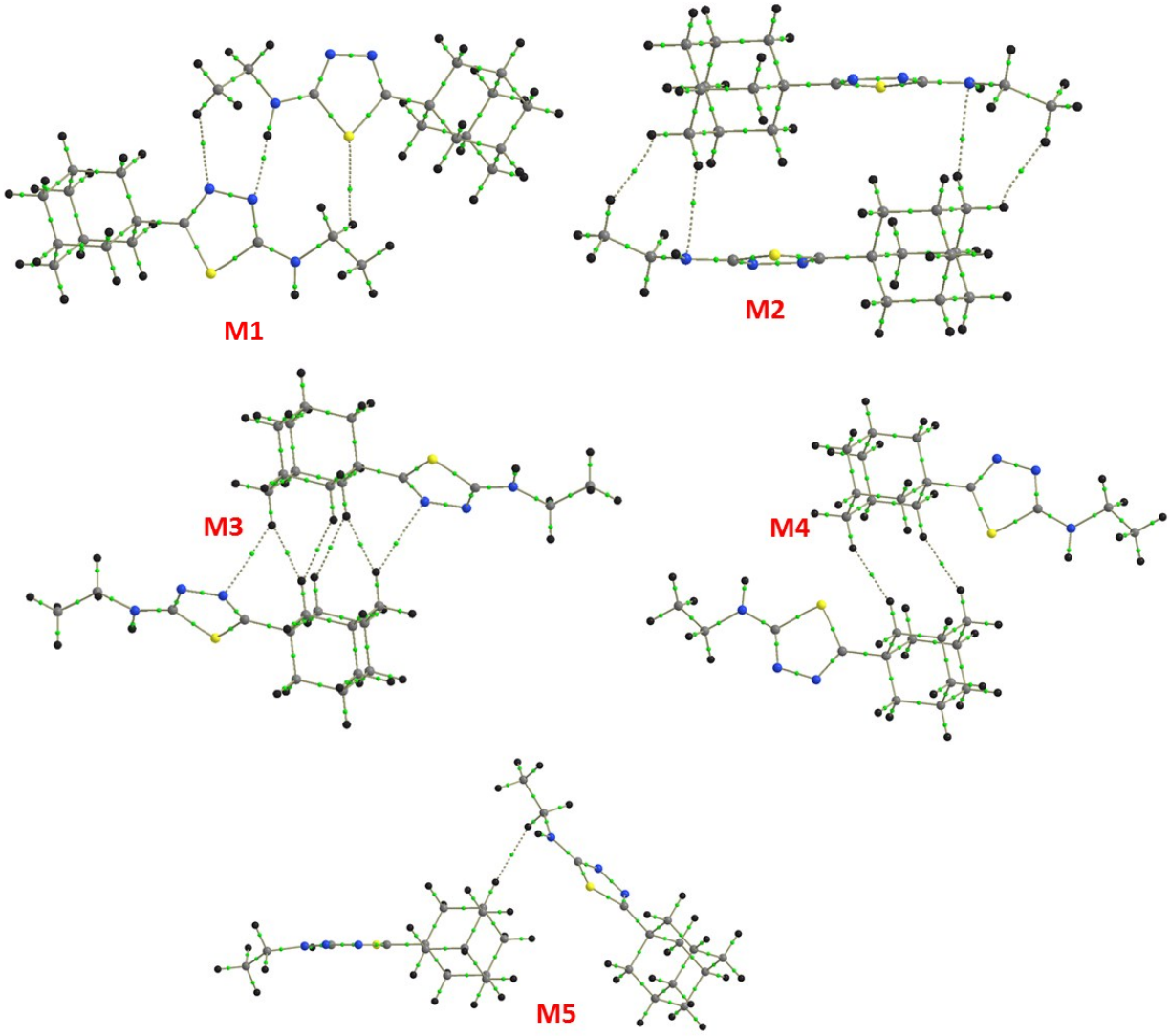

Fig. S9. Molecular graphs showing the existence of intermolecular interactions in dimers of M1-M5 in compound **I**.

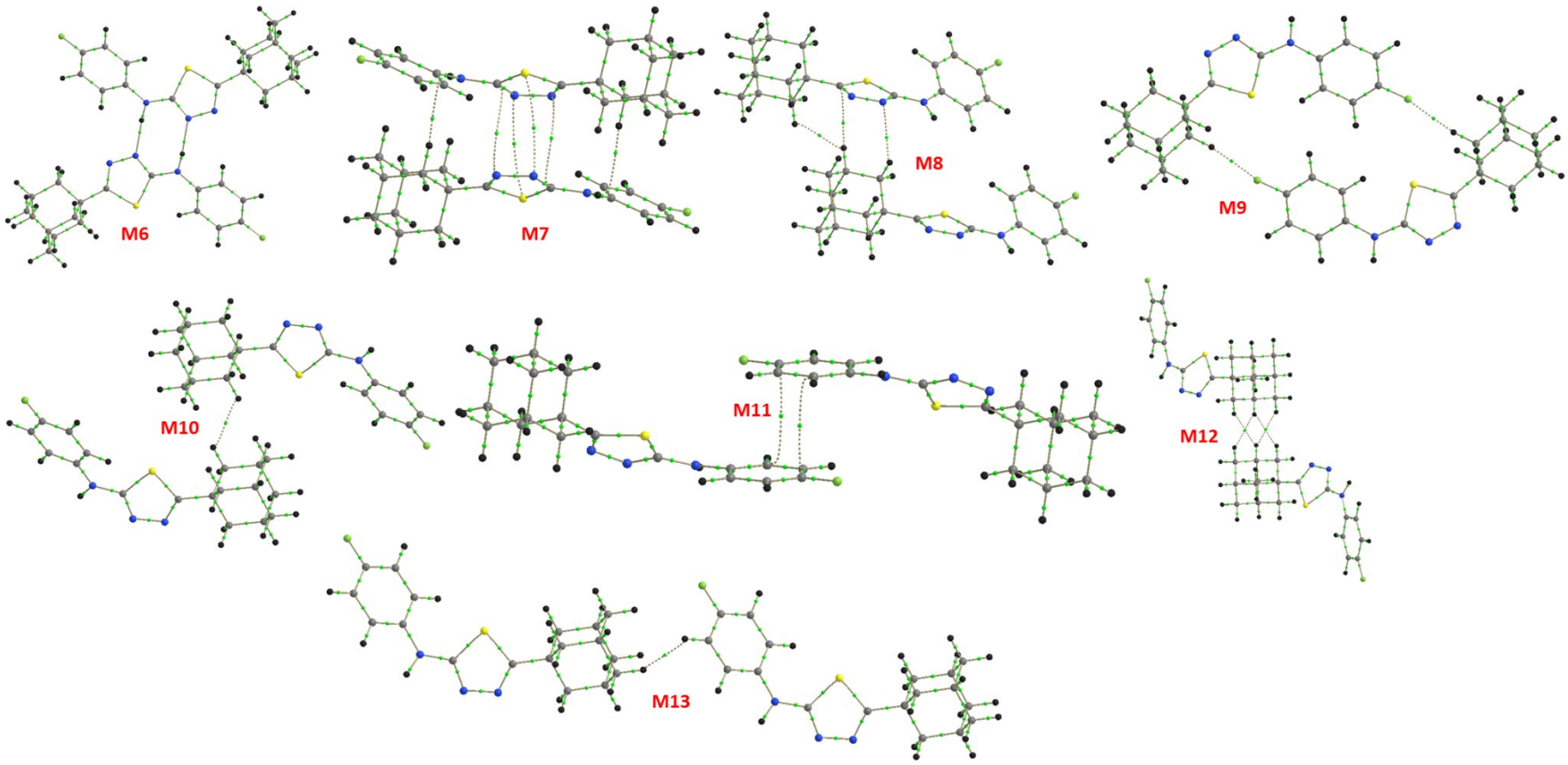

Fig. S10. Molecular graphs showing the existence of intermolecular interactions in dimers of M6-M13 in **II**.

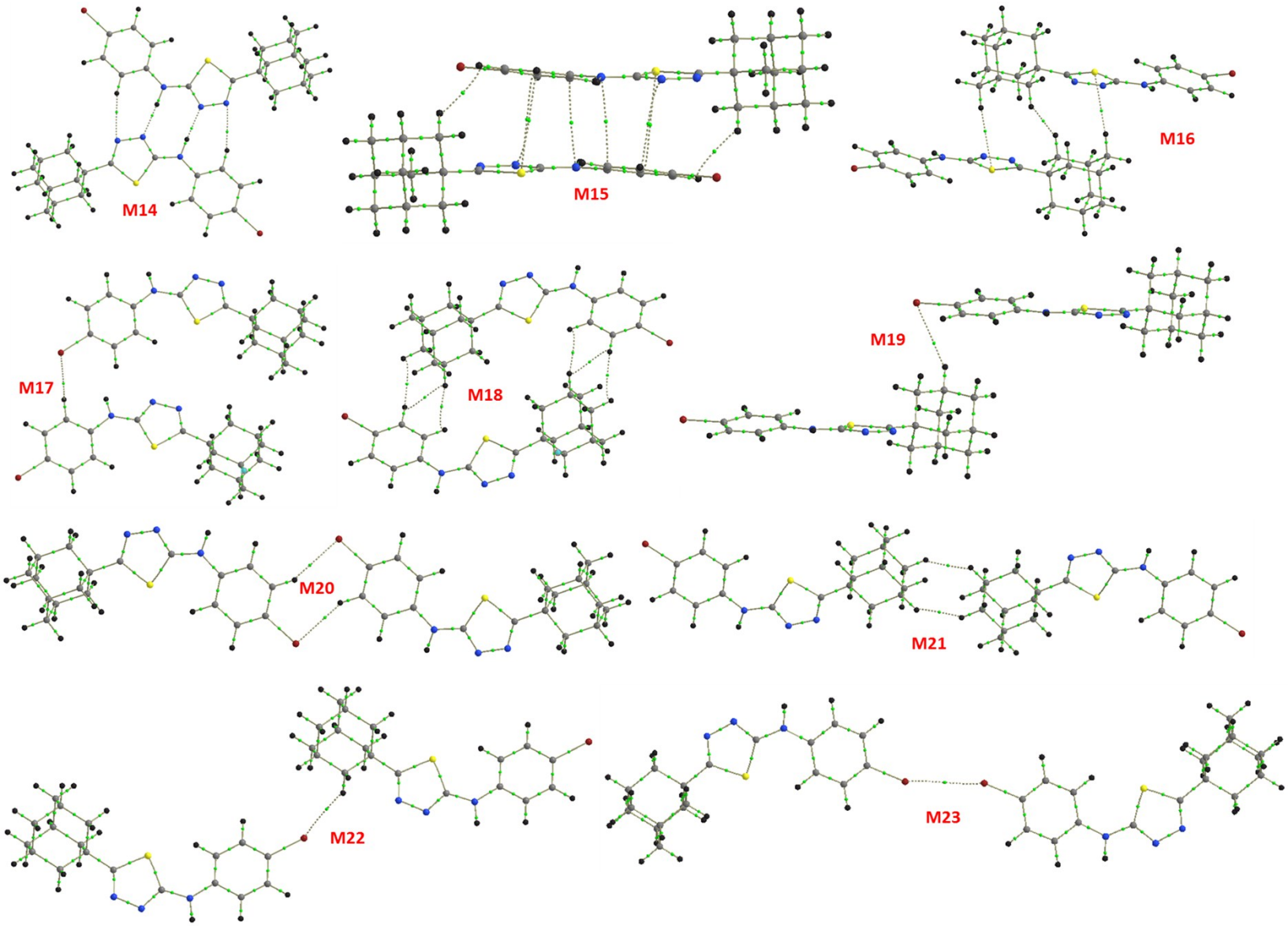

Fig. S11. Molecular graphs showing the existence of intermolecular interactions in dimers of M14-M23 in **III**.